

Sequence Matters: Modulating Electronic and Optical Properties of Conjugated Oligomers via Tailored Sequence

Benjamin N. Norris,[†] Shaopeng Zhang,[‡] Casey M. Campbell,[§] Jeffrey T. Auletta,[‡] Percy Calvo-Marzal,[‡] Geoffrey R. Hutchison,^{‡,*} and Tara Y. Meyer^{‡,*}

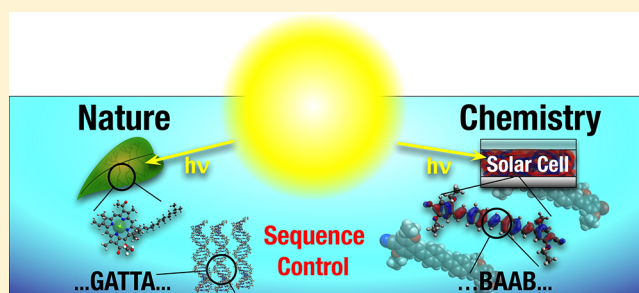
[†]Department of Chemistry, Frostburg State University, 101 Braddock Road, Frostburg, Maryland 21532, United States

[‡]Department of Chemistry, University of Pittsburgh, 219 Parkman Avenue, Pittsburgh, Pennsylvania 15260, United States

[§]School of Chemistry and Biochemistry, Georgia Institute of Technology, 901 Atlantic Drive, Atlanta, Georgia 30332-0400, United States

S Supporting Information

ABSTRACT: Although sequence must necessarily affect the photophysical properties of oligomers and copolymers prepared from donor and acceptor monomers, little is known about this effect, as nearly all the donor/acceptor materials have an alternating structure. A series of sequenced *p*-phenylene–vinylene (PV) oligomers was synthesized and investigated both experimentally and computationally. Using Horner–Wadsworth–Emmons (HWE) chemistry, a series of dimers, trimers, tetramers, pentamers, and hexamers were prepared from two building block monomers, a relatively electron-poor unsubstituted *p*-phenylene–vinylene (A) and an electron-rich dialkoxy-substituted *p*-phenylene–vinylene (B). UV–vis absorption/emission spectra and cyclic voltammetry demonstrated that the optoelectronic properties of these oligomers depended significantly on sequence. Calculations predicting the HOMO–LUMO gap of the sequenced oligomers correlated well with the experimental properties for the 2- to 4-mers, and the consensus model developed was used to design hexameric sequences with targeted characteristics. Despite the weak acceptor qualities of the “A” monomer employed in the study, HOMO–LUMO gap differences of ~ 0.25 eV were found for isomeric, sequenced oligomers. In no case did the alternating structure give the largest or smallest gap. The use of sequence as a strategy represents a new dimension in tailoring properties of π -conjugated polymers.



INTRODUCTION

Nature refines the properties of biopolymers, not just by composition, but also by orchestration of monomer sequence. For example, the photosynthetic pathway exhibits optical absorption, energy transfer, electron transfer, and chemical transformation motifs all within a self-assembled package.¹ In stark contrast, efforts to synthesize organic solar cells focus almost solely on chemical variation of monomer structure, seeking to derive optimal optical, energetic, and charge transfer properties using a very limited number of patterns.^{2–4} Organic photovoltaics promise to significantly reduce the cost of solar electrical generation, so optimization of the material should be driven by sequence as well as composition. Here we demonstrate by combined synthesis, computational design, and optical and electrochemical characterization that altering the sequence of widely studied conjugated phenylene–vinylene oligomers can significantly modulate both optical and redox properties. We show that neither long block nor alternating sequences will likely yield optimal properties for photovoltaics.

Third generation photovoltaic polymers rely on the donor–acceptor approach in which electron-poor acceptor and electron-rich donor monomers are copolymerized in an effort

to engineer the desired optoelectronic properties as a hybrid of the properties of the respective homopolymers.^{2–9} Although alternating and random copolymers/oligomers containing a variety of donor and acceptor monomers have been prepared,^{2,10–13} no systematic effort has been made to determine the effect of the donor–acceptor sequence on the optoelectronic properties. For example, units that encode sequence in some form are nearly always symmetric^{14–20} and there are only a few studies that include more than two examples of materials that have complex sequences²¹ or are isomeric but sequentially diverse.^{22,23}

Recent results from our groups suggest that monomer sequence can have as much influence on properties of relevance to photovoltaics as the identities and ratios of the monomers. We developed a genetic algorithm for surveying the structure space of conjugated oligomers assembled from various donor–acceptor dimers and computationally predicted the power-conversion efficiencies of photovoltaic cells.²⁴ Oligomers with complex sequences of dimers exhibited surprisingly large

Received: January 18, 2013

Published: February 11, 2013

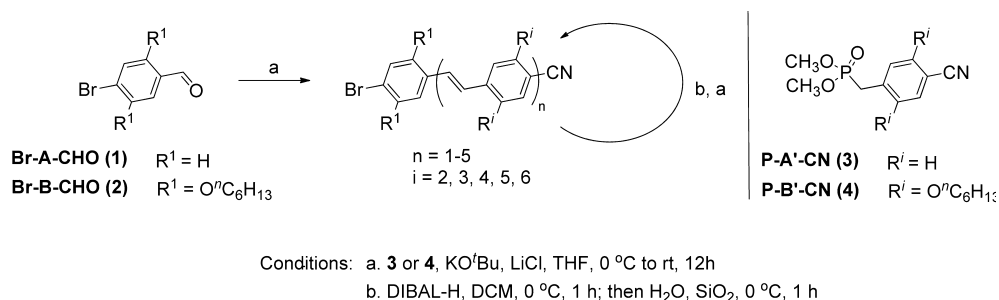


Figure 1. Synthetic approach to sequenced oligomers.

differences in optoelectronic properties and photovoltaic efficiencies.

The power of sequence to control oligomer and polymer properties in applications other than photovoltaics is increasingly being investigated.^{25–27} We have, for example, examined the effects of sequence on the properties of poly(lactic-*co*-glycolic acid)s and poly(fluorene-*co*-methylene)s.^{28–33} The power of sequence to control the properties of oligomers and polymers can also be seen in the metal-catalyzed control of stereochemistry in polyolefins,³⁴ poly lactides,^{11,17} and other monomers³⁵ and convergent/divergent assembly of precise oligomers,³⁶ sequential polycondensation,³⁷ acyclic diene metathesis,³⁸ controlled free-radical polymerizations,^{39–42} and template synthesis of sequences.⁴³

We report herein a model study, combining synthesis and characterization of sequenced oligomers and computational design, that demonstrates the power of sequence to control optoelectronic properties. The interplay between the experimental and theoretical work is synergistic throughout. Experimental results from the synthesis of a library of easily prepared shorter oligomers were used to verify our computational approach. The experimental trends and calculations were then exploited to design targeted hexamers. Computational screening of the sequences proved critical as the longer oligomers are synthetically complex and difficult to survey experimentally due to the exponential increase in possible combinations with oligomer length.

RESULTS

Synthesis of Sequenced Oligomers. Oligo(phenylene-vinylene)s (OPVs) were targeted for this sequence study because these oligomers are well-known to have varied, substituent-dependent optoelectronic properties.^{9,23} A variety of methods for preparation of OPVs have been reported by our group and other researchers.^{21,23,44–46} The approach selected for this study was a modification of the synthesis by Jørgensen and Krebs⁴⁷ featuring alternating Horner–Wadsworth–Emmons (HWE) olefinations of a *p*-cyanobenzyl phosphonate monomer with an oligomer aldehyde followed by DIBAL-H reduction to yield a new reactive aldehyde (Figure 1). The key differences in our approach are the iterative coupling of single phenylene units, rather than dimeric units, which allows for the synthesis of oligomers of any length and pattern, and the use of nitrile-terminated units rather than acetals, which increased both the *E*-selectivity of the HWE reaction and the ease of purification of the oligomers.

The following naming conventions are employed throughout: (1) unsubstituted *p*-phenylene units are designated **A**; (2) dialkoxy-substituted units are designated **B**; (3) **A'** and **B'** are used for *p*-phenylene units bearing the conjugated cyano end

group; (4) oligomers are labeled dimer, trimer, etc. based on the number of phenyl units (rather than complete phenylene–vinylene units) to avoid the use of the more exact but cumbersome *n*.5-mer terminology.

In our initial investigations we encountered low stereoselectivity when using acetal-protected monomers—a perplexing result given the lack of discussion of stereoselectivity in reports of previous syntheses using the HWE reaction. Our model reactions involved the HWE reaction between alkoxy-substituted bromobenzaldehyde **Br-B-CHO** and either alkoxy-substituted phosphonate monomer **P-B'-CN** (**4**) or the derivative in which the terminal cyano is replaced with an acetal, which we expected to be the most difficult HWE combinations for steric reasons, to give the alkoxy-substituted dimers. The reaction with the acetal-protected monomer (Table 1, entry 1) proceeded in quantitative yield and without

Table 1. Stereoselectivity of HWE Reactions^a

Entry	R	Additive	Yield	<i>E</i> : <i>Z</i> ^a
1		None	100%	2:1
2		LiCl	55%	4:1
3	CN	None	70%	5:1
4	CN	LiCl	100%	>9:1

^a*E*:*Z* determined by ¹H NMR spectroscopy.

loss of the bromine atom, as reported by Jørgensen and Krebs.⁴⁷ This reaction, however, gave the dimer as a 2:1 mixture of *E* and *Z* isomers. As these isomers are difficult to separate by chromatography, we pursued further modifications. Addition of LiCl, which has been shown to increase *E*-selectivity in HWE reactions,^{48,49} increased the selectivity to 4:1 *E*:*Z* at the expense of conversion and yield (Table 1, entry 2). Nitrile monomer **2** (Table 1, entry 3) gave **Br-BB'-CN** in a 70% yield with higher *E*-selectivity (5:1). Addition of LiCl to this reaction increased both the yield to 100% and the *E*-selectivity to >9:1. Additionally, the CN-terminated oligomers were more easily purified by chromatography.

Four dimers, **Br-AA'-CN**, **Br-AB'-CN**, **Br-BA'-CN**, and **Br-BB'-CN** were prepared by this procedure in high yields and *E*-selectivities (Table 2). The nitrile group of each dimer could then be reduced with DIBAL-H to produce an aldehyde end group that allowed for subsequent HWE reactions to increase chain length. By repeating successive cycles of nitrile reduction and HWE coupling a total of 22 sequenced oligomers were

Table 2. Sequenced Oligophenylene Vinylenes

oligomer	R ¹	R ²	R ³	R ⁴	R ⁵	R ⁶	% yield ^a	E:Z ^b
Br-AA'-CN	H	H	—	—	—	—	85 ^c	>20:1 ^d
Br-AB'-CN	H	O ⁿ C ₆ H ₁₃	—	—	—	—	92 ^c	20:1
Br-BA'-CN	O ⁿ C ₆ H ₁₃	H	—	—	—	—	96 ^c	20:1
Br-BB'-CN	O ⁿ C ₆ H ₁₃	O ⁿ C ₆ H ₁₃	—	—	—	—	96 ^c	9:1
Br-AAB'-CN	H	H	O ⁿ C ₆ H ₁₃	—	—	—	78	20:1
Br-BAA'-CN	O ⁿ C ₆ H ₁₃	H	H	—	—	—	93	20:1
Br-BAB'-CN	O ⁿ C ₆ H ₁₃	H	O ⁿ C ₆ H ₁₃	—	—	—	89	20:1
Br-ABA'-CN	H	O ⁿ C ₆ H ₁₃	H	—	—	—	87	9:1
Br-ABB'-CN	H	O ⁿ C ₆ H ₁₃	O ⁿ C ₆ H ₁₃	—	—	—	82	8:1
Br-BBA'-CN	O ⁿ C ₆ H ₁₃	O ⁿ C ₆ H ₁₃	H	—	—	—	79	8:1
Br-BAAB'-CN	O ⁿ C ₆ H ₁₃	H	H	O ⁿ C ₆ H ₁₃	—	—	83	>20:1 ^d
Br-ABAB'-CN	H	O ⁿ C ₆ H ₁₃	H	O ⁿ C ₆ H ₁₃	—	—	71	>20:1 ^d
Br-BABA'-CN	O ⁿ C ₆ H ₁₃	H	O ⁿ C ₆ H ₁₃	H	—	—	85	>20:1 ^d
Br-BBAA'-CN	O ⁿ C ₆ H ₁₃	O ⁿ C ₆ H ₁₃	H	H	—	—	98	>20:1 ^d
Br-AABB'-CN	H	H	O ⁿ C ₆ H ₁₃	O ⁿ C ₆ H ₁₃	—	—	80	20:1
Br-ABBA'-CN	H	O ⁿ C ₆ H ₁₃	O ⁿ C ₆ H ₁₃	H	—	—	73	>20:1 ^d
Br-AABBB'-CN	H	H	O ⁿ C ₆ H ₁₃	O ⁿ C ₆ H ₁₃	O ⁿ C ₆ H ₁₃	—	59	10:1
Br-BABAB'-CN	O ⁿ C ₆ H ₁₃	H	O ⁿ C ₆ H ₁₃	H	O ⁿ C ₆ H ₁₃	—	90	>20:1 ^d
Br-BBAAA'-CN	O ⁿ C ₆ H ₁₃	O ⁿ C ₆ H ₁₃	H	H	H	—	88	>20:1 ^d
Br-AABBBBA'-CN	H	H	O ⁿ C ₆ H ₁₃	O ⁿ C ₆ H ₁₃	O ⁿ C ₆ H ₁₃	H	66	9:1
Br-BABABBA'-CN	O ⁿ C ₆ H ₁₃	H	O ⁿ C ₆ H ₁₃	H	O ⁿ C ₆ H ₁₃	H	74	>20:1 ^d
Br-BBAAAAB'-CN	O ⁿ C ₆ H ₁₃	O ⁿ C ₆ H ₁₃	H	H	H	O ⁿ C ₆ H ₁₃	60	>20:1 ^d

^aYield over two steps from relevant previous oligomer (e.g., Br-BBAA'-CN was prepared from Br-BBA'-CN), unless noted. ^bEstimated from ¹H NMR spectra. ^cYield over one step from Br-A-CHO (1) or Br-B-CHO (2). ^dNo peaks for Z isomers were observed.

Table 3. Optoelectronic Properties of Sequenced OPVs

oligomer	$\lambda_{\max}^{\text{abs } a} / \text{nm}$	$\epsilon^b / 10^{-3} \text{ cm}^{-1} \text{ M}^{-1}$	$\lambda_{\max}^{\text{em } a} / \text{nm}$	$\lambda_{\max}^{\text{em } c} / \text{nm}$	$\Delta E_{\text{gap}}^{\text{opt } d} / \text{eV}$	$E_{\text{peak}}^{\text{ox } e} / \text{V}$	$E_{\text{peak}}^{\text{red } e} / \text{V}$	$\Delta E_{\text{gap}}^{\text{ec } f} / \text{eV}$
Br-AA'-CN	327	54.5	379	463	3.44	1.45	-1.93	3.38
Br-BA'-CN	309, 362	28.1, 29.2	450	460	2.97	1.06	-1.96	3.02
Br-AB'-CN	316, 364	29.4, 24.9	418	443	2.99	1.23	-1.94	3.17
Br-BB'-CN	303, 380	16.9, 26.6	450	519	2.89	1.06	-2.17	3.23
Br-AAB'-CN	385	93.2	433	507	2.86	1.06	-1.94	3.00
Br-BAA'-CN	383	73.2	476	497	2.84	0.95	-1.93	2.88
Br-BAB'-CN	396	72.4	474	504	2.77	0.97	-1.97	2.94
Br-ABA'-CN	334, 406	37.9, 50.2	477	514	2.65	0.84	-1.92	2.76
Br-ABB'-CN	329, 412	34.0, 53.8	478	524	2.63	0.81	-1.93	2.74
Br-BBA'-CN	333, 412	29.4, 53.9	488	522	2.62	0.78	-1.94	2.72
Br-BAAB'-CN	408	93.3	485	512	2.72	0.87	-1.94	2.81
Br-ABAB'-CN	422	73.9	499	549	2.58	0.69	-2.02	2.71
Br-BABA'-CN	425	89.9	492	534	2.56	0.69	-1.98	2.67
Br-BBAA'-CN	366, 424	41.4, 86.2	515	553	2.56	0.65	-1.99	2.64
Br-AABB'-CN	360, 425	47.9, 83.7	492	547	2.55	0.70	-1.99	2.69
Br-ABBA'-CN	337, 437	35.3, 78.3	511	541	2.47	0.67	-1.95	2.62
Br-AABBB'-CN	351 449	35.5, 90.7	522	578	2.43	0.63	-1.97	2.60
Br-BABAB'-CN	435	97.7	508	557	2.52	0.70	-1.96	2.66
Br-BBAAA'-CN	427	78.1	500	583	2.56	0.69	-1.96	2.65
Br-AABBBBA'-CN	342 462	40.8, 94.0	538	616	2.29	0.54	-1.92	2.46
Br-BABABBA'-CN	448	112.2	509	580	2.46	0.64	-1.94	2.58
Br-BBAAAAB'-CN	430	108	494	566	2.53	0.67	-1.99	2.66

^aMeasured in $\sim 10^{-6}$ M chloroform solution. ^bCalculated at $\lambda_{\max}^{\text{abs}}$. ^cThin film, cast from chloroform solution. ^dDetermined at the onset of the absorption spectrum. ^ePotential vs Ag/Ag⁺, 240 μM in 0.1 M Bu₄NPF₆ in THF. ^fDetermined as $\Delta E_{\text{gap}}^{\text{ec}} = e(E_{\text{peak}}^{\text{ox}} - E_{\text{peak}}^{\text{red}})$.

prepared: four dimers, six trimers, six tetramers, three pentamers, and three hexamers. All HWE reactions and DIBAL-H reductions used to prepare the trimers and tetramers proceeded in good to excellent yields. The yields of the pentamers and hexamers were lower in some cases due to the decreased solubility of the longer oligomers. All oligomers were prepared with high (>8:1) *E:Z*-selectivity, with the lowest selectivity observed for those oligomers with two or more adjacent **B** units. In many cases, the *Z*-isomers were not observable by NMR after purification which suggests an upper limit of 3–5% contamination. In order to facilitate further elaboration of the oligomers, including the possibility of incorporating them into polymeric materials in the future, each OPV was prepared with a bromide group on one terminus and a nitrile on the other.

Computational Approach. Computational methods offer an easy mechanism to screen optoelectronic properties of π -conjugated materials.^{50–55} While density functional theory (DFT) computed orbital eigenvalues are nonphysical,^{56,57} numerous studies have found a high degree of correlation between these energies and vertical ionization potentials and electron affinities^{58,59} as well as accurate predictions of optical band gaps.⁵⁰ For solution electrochemistry, the redox potentials can be determined based on the free energy change,^{60,61} such as the adiabatic difference in total energy between the neutral and charged systems (Δ SCF). In many cases, systematic deviations reflect a linear free energy relationship⁶² between computed and experimental properties, which can be captured simply by linear regression. This regression also corrects for other errors, such as differences in computed and experimental conformations.

Since our objective was to reliably and accurately screen for targeted properties of sequenced oligomers, we sought to extend these regression techniques by use of a “consensus model” to minimize both systematic and random errors, i.e., to improve accuracy and correlation. The consensus model employed here combines two different computational predictions of an experimental property using multivariate regression, e.g., oxidation potential. For redox potentials, DFT eigenvalues and adiabatic total energy differences (Δ SCF) were used, and for optical absorption energies and oscillator strengths, ZINDO and time-dependent DFT (TDDFT) methods were combined.

The computational method was originally developed and calibrated using optical and electrochemical data from sequenced 2-, 3-, and 4-mers. The method was then used to predict the properties of all possible hexamer sequences with a 1:1 A:B ratio (Supporting Information, Table S5). Using these data, three hexamers with specifically targeted behavior, **Br-AABBBA'-CN**, **Br-BBAAAB'-CN** and **Br-BABABA'-CN**, were selected for synthesis. Prior to discussing the computational results/predictions in more detail, however, the characterization data for all oligomers are presented.

Optical Spectroscopy. The optical spectra of the oligomers vary significantly with sequence (Table 3, Figure 2, and Supporting Information for all spectra). The absorption maxima of both the trimer and tetramer series vary over a range of ~30 nm. The HOMO–LUMO gaps, estimated at the onset of absorption, vary over a range ~0.25 eV.

Among the trimers, band gap decreases with decreasing **A** content, which is consistent with previous reports.²⁰ Sequence is still an important factor, however; **Br-ABA'-CN** exhibits a smaller gap than **Br-BAB'-CN**, despite the latter having more **B**

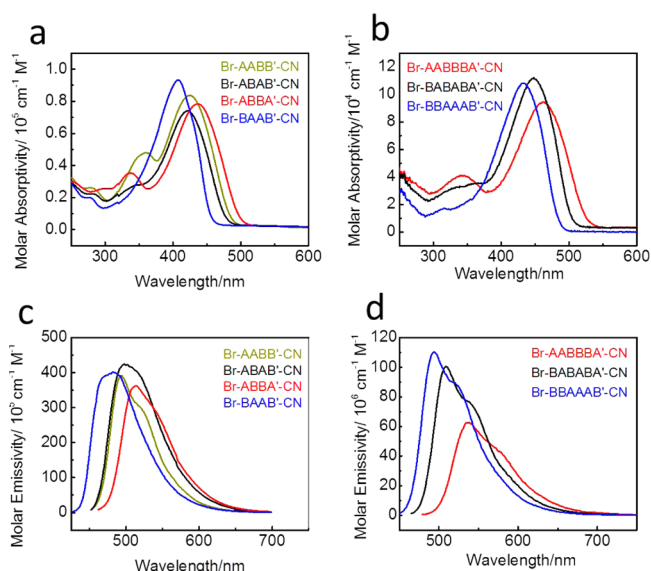


Figure 2. Absorption and emission spectra in CHCl_3 (10^{-6} M): (a) absorption spectra for selected tetramers; (b) absorption spectra for hexamers; (c) emission spectra for selected tetramers; (d) emission spectra for hexamers.

units. The emission maximum in both solution and thin film follow a similar trend to $\lambda_{\text{max}}^{\text{abs}}$. There is, however, a noticeable red shift in the solid state that is consistent with aggregation.^{63,64}

The absorption spectra of **Br-ABBA'-CN**, **Br-BAAB'-CN**, and a representative alternating (**Br-BABA'-CN**) and blocky (**Br-AABB'-CN**) sequence are presented in Figure 2a. Among the tetramers, the sequence with the smallest band gap is **Br-ABBA'-CN**, while the complementary sequence, **Br-BAAB'-CN**, exhibits the largest. The alternating sequences (**Br-ABAB'-CN** and **Br-BABA'-CN**) and the blocky sequences (**Br-AABB'-CN** and **Br-BBAA'-CN**) are intermediate. The effect of *Z*-isomer contamination on the optical spectra is negligible, as the materials were prepared with high *E*-selectivity (*vide infra*).

Sequence also impacts the absorption profile of the oligomers. Several sequences exhibit a well-separated higher energy absorption band. These tended to be sequences with **AA** or **BB** blocks, for example **Br-BBAA'-CN** or **Br-ABBA'-CN**, among the tetramers. While the longer wavelength absorptions are primarily π – π^* transitions delocalized across the entire oligomer, the higher energy, weaker absorptions likely derive from excitations between **BB** and **AA** blocks. These peaks, which were also found in the computational results, arise from shorter geometric distances and, thus, exhibit smaller transition dipole moments.

Although the range of band gaps for the pentamer series is small (0.13 eV), the range for the hexamer series is large (0.24 eV), similar to the tetramer series. The sequence **Br-AABBBA'-CN** exhibits the smallest band gap while the complementary sequence **Br-BBAAAB'-CN** has the largest. The alternating hexamer **Br-BABABA'-CN** exhibits intermediate properties, as predicted (*vide supra*).

Electrochemistry. The electrochemistry of the oligomers is also strongly dependent on sequence (Figure 3, Table 3 and Supporting Information for the complete data set). All oligomers with sequences containing multiple **B** units exhibit multiple oxidation peaks in their differential pulse voltammograms (DPVs). The first oxidation potentials of the oligomers

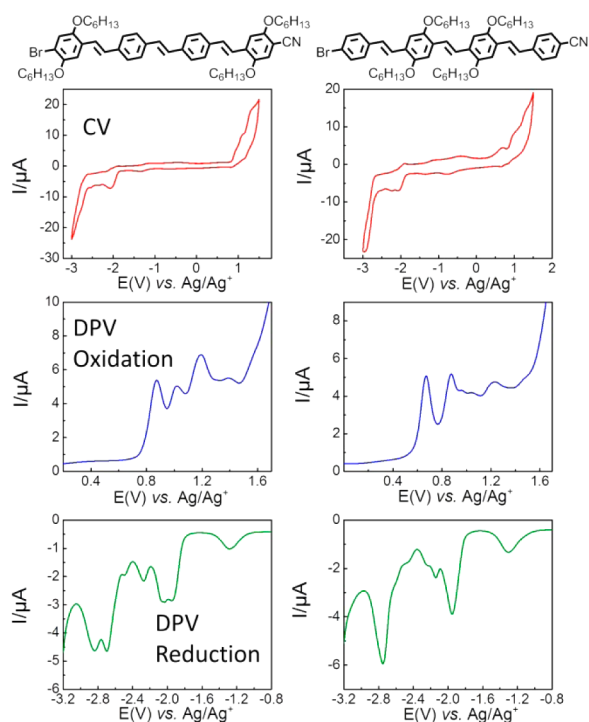


Figure 3. Cyclic voltammograms and differential pulse voltammograms of Br-BAAB'-CN and Br-ABBA'-CN in THF.

demonstrate clear dependence on sequence and follow similar trends to the absorption maxima.

The first oxidation potentials of the trimers depend partly on composition, with Br-AAB'-CN and Br-BAA'-CN exhibiting higher first oxidations than Br-ABB'-CN and Br-BBA'-CN, due to higher A unit concentration. This effect reverses for the other two trimers. The number of oxidation peaks and the shapes of the oxidation profiles clearly demonstrate sequence dependence as well, although there is not an obvious trend. The reduction potentials show little dependence on sequence, composition, or conjugation length. With few exceptions, the first reduction potential is at ca. -1.90 V vs Ag/Ag⁺, likely due to reduction of the cyano group.

For the tetramer series, the first oxidation potentials vary over a range of ~ 200 mV in THF, with Br-BAAB'-CN exhibiting the highest first oxidation potential, and the complementary Br-ABBA'-CN exhibiting a much lower oxidation potential (0.87 and 0.67 V vs Ag/Ag⁺, respectively). The alternating and blocky sequenced tetramers fall in between, with one exception; Br-BBAA'-CN exhibits the least positive first oxidation potential.

The electrochemical HOMO–LUMO gaps, $\Delta E_{\text{gap}}^{\text{ec}}$, follow similar patterns to the first oxidation potentials since the first reduction potentials exhibit minimal variation. In contrast to the optical band gaps, the electrochemical gaps exhibit greater variation with sequence. In four out of five pairs of reverse sequences (for example, Br-ABB'-CN and Br-BBA'-CN), the B-first sequence exhibits a lower gap than the A-first sequence. A high degree of correlation was otherwise observed between electrochemical and spectroscopic gaps ($R^2 = 0.92$).

We find a similar trend in the redox potentials of the hexamers as was found in the optical spectroscopy. The sequence Br-AABBBA'-CN exhibits the lowest oxidation potential and smallest $\Delta E_{\text{gap}}^{\text{ec}}$, while the complementary sequence Br-BBAAAB'-CN has the highest oxidation potential

and largest $\Delta E_{\text{gap}}^{\text{ec}}$. The alternating hexamer Br-BABABA'-CN exhibits intermediate properties. The range of gaps is 0.2 eV, in close agreement with the spectroscopic range of 0.24 eV.

Thermal Properties. Although not targeted for computational prediction in this investigation, the thermal properties of the prepared oligomers were also acquired and found to depend on sequence (Figure 4, Table 4). All oligomers were

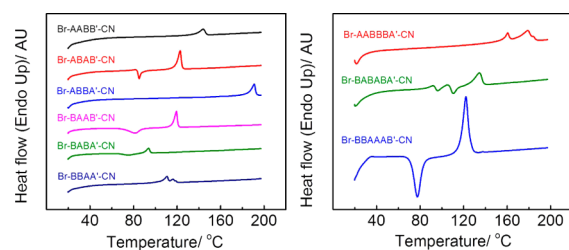


Figure 4. DSC thermograms of all six sequenced tetramers and all three sequenced hexamers.

Table 4. Thermal Properties of the Sequenced OPVs

oligomer	$T_{\text{iso}}^a / ^\circ\text{C}$	$T_{\text{LC}}^a / ^\circ\text{C}$	$T_{\text{C}}^b / ^\circ\text{C}$
Br-AA'-CN	197	—	151, 167
Br-BA'-CN	83.2	—	30.6
Br-AB'-CN	74.7 ^c	—	—
Br-BB'-CN	96.3	—	68.8
Br-AAB'-CN	105	—	41.6
Br-BAA'-CN	125 ^c	—	—
Br-BAB'-CN	104	—	77.8
Br-ABA'-CN	185	64.8 ^c	79.5, 85.3, 92.7
Br-ABB'-CN	114	—	43.2
Br-BBA'-CN	109	—	—
Br-BAAB'-CN	119	81.2	—
Br-ABAB'-CN	123	85.0	41.7
Br-BABA'-CN	94	75.4	—
Br-BBAA'-CN	116	111	57.5
Br-AABB'-CN	144	66.3 ^c	114, 121
Br-ABBA'-CN	191	—	124
Br-AABBB'-CN	169	160	156
Br-BABAB'-CN	130	110	106
Br-BBAAA'-CN	171	86.2 ^c	153
Br-AABBBA'-CN	184	178, 161	165, 169
Br-BABABA'-CN	134	92, 105	55.3
Br-BBAAAB'-CN	122	—	—

^aExothermic transition observed on second heating scan. ^bExothermic transition observed on second cooling scan. ^cTransition observed in first scan only.

crystalline with melting points (T_{iso}) ranging from 80 to 170 °C and most exhibited clear crystallization exotherms (T_{C}) during differential scanning calorimetry (DSC). Oligomers with two unsubstituted terminal A monomers, Br-AA'-CN, Br-ABA'-CN, Br-ABBA'-CN, etc. exhibited higher temperature melting transitions than other sequences of the same length. Multiple melting transitions observed for several of the longer oligomers are consistent with the existence of liquid crystalline phases with narrow ranges of stability.

Comparison of Computed and Experimental Data. As stated above, the computational consensus models were calibrated by the experimental results on the 2-, 3-, and 4-mers. In general, computed properties (Table 5) show only

Table 5. Computed First Oxidation and Reduction Peak Potentials and Optical Excitation Energies $\Delta E_{\text{gap}}^{\text{comp}}$ of Sequenced OPVs from Consensus Models

oligomer	predicted E^{ox}/eV	predicted E^{red}/eV	$\Delta E_{\text{gap}}^{\text{comp}}/\text{eV}$
Br-AA'-CN	1.43	-1.97	3.41
Br-BA'-CN	1.13	-1.99	3.12
Br-AB'-CN	1.21	-1.99	3.20
Br-BB'-CN	1.03	-2.00	3.03
Br-AAB'-CN	1.01	-1.97	2.97
Br-BAA'-CN	0.96	-1.97	2.93
Br-BAB'-CN	0.88	-1.98	2.85
Br-ABA'-CN	0.89	-1.96	2.85
Br-ABB'-CN	0.84	-1.99	2.82
Br-BBA'-CN	0.81	-1.97	2.78
Br-BAAB'-CN	0.80	-1.96	2.76
Br-ABAB'-CN	0.75	-1.95	2.70
Br-BABA'-CN	0.72	-1.95	2.67
Br-BBAA'-CN	0.73	-1.95	2.67
Br-AABB'-CN	0.76	-1.96	2.72
Br-ABBA'-CN	0.69	-1.96	2.65
Br-AABBB'-CN	0.62	-1.97	2.58
Br-BABAB'-CN	0.65	-1.96	2.61
Br-BBAAA'-CN	0.66	-1.94	2.61
Br-AABBBA'-CN	0.54	-1.97	2.51
Br-BABABA'-CN	0.61	-1.95	2.56
Br-BBAAAB'-CN	0.62	-1.96	2.59

small residual errors compared to their experimental counterparts. The main exception is the predicted LUMO energies or $\Delta\text{SCF}(-)$ values, compared to the electrochemical first reduction potentials, which are largely dominated by the localized cyano reduction. DFT calculations predict, incorrectly, that the LUMOs are strongly delocalized across the entire oligomer (Supporting Information, Figure S72 for the tetramers).

We find mean unsigned errors (MUE) between computed and experimental parameters after the linear regression analysis to be very low, as illustrated in Figure 5, with ~ 0.04 eV MUE for oxidation potentials ($R^2 = 0.96$), ~ 0.04 eV MUE for reduction potentials, ~ 0.07 eV MUE for optical excitation energies ($R^2 = 0.89$), and $\sim 10\%$ MUE for optical absorption extinction coefficients ($R^2 = 0.94$). The high degree of agreement is not surprising because the sequenced oligomers define a closely analogous series, and the consensus technique minimizes systematic and random errors.

On the basis of these consensus models, we predicted properties of all 20 sequenced hexamers prior to their synthesis (Supporting Information, Table S5), and found distinct differences, despite the subtle variation in electronic structure of the B and A monomers. Br-AABBBA'-CN was predicted to exhibit the lowest HOMO energy and one of the smallest optical band gaps, while the complementary sequence Br-BBAAAB'-CN had a higher HOMO energy and gap. The

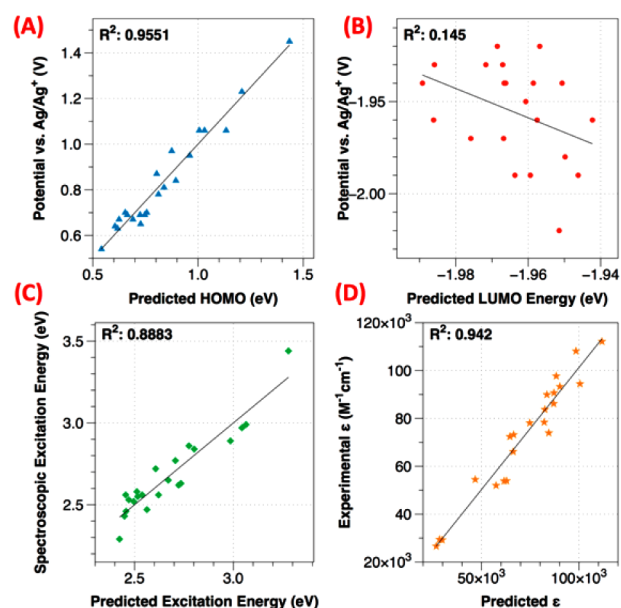


Figure 5. Correlations between computed (a) first oxidation potential, (b) first reduction potential, (c) optical excitation energies $\Delta E_{\text{gap}}^{\text{comp}}$, and (d) extinction coefficients with their experimental counterparts. Note that for all predicted properties, a consensus model of two predictors was used.

conventional alternating sequences Br-ABABAB'-CN and Br-BABABA'-CN fell in between. As observed experimentally, these predictions proved relatively correct, although the difference in the experimental band gaps between hexamers was larger than that predicted. The calculated difference in predicted gaps spanned a range of only 0.05 eV, while the experimental gaps spanned 0.2 and 0.24 eV for optical and electrochemical data, respectively.

There are several possible explanations for this difference. It is well-known that using TDDFT with conventional functionals underestimates band gaps in longer oligomers due to incorrect asymptotic behavior. For this reason, when screening the hexamers, we solely used ZINDO calculations. Also, such behavior has been observed previously and attributed to differences in computed and experimental conformations.^{65,66} The calculations were performed on a low energy conformation, tending toward planarity in longer oligomers, not a solution ensemble of different conformations with shorter effective conjugation lengths.⁶⁶ This effect likely explains the smaller range in predicted band gaps in the hexamers, compared with experiment. Still, sequence determines both the orbital overlap and partial charge transfer between B and A monomers involved in the electronic excitations, and also dictates conformation in solution.³¹

DISCUSSION

Using an iterative strategy, we prepared multiple unsymmetric *p*-phenylene–vinylene oligomers that differ only in sequence. *E:Z* selectivity in the key HWE coupling was improved by using a nitrile precursor for the aldehyde, in lieu of the more commonly exploited acetal. The product oligomers bear functional end groups that allow for further elaboration including potential inclusion as units in a repeating sequence copolymer. Characterization of these oligomers establishes that the optical absorption and emission energies and intensities,

first oxidation potentials, and thermal properties were all modulated by sequence.

Our computational approach predicted the sequence-based optoelectronic properties of the conjugated oligomers with outstanding agreement. We were able, as a result, to selectively prepare longer oligomers with targeted characteristics. In particular, we both predicted and confirmed by synthesis that the oxidation potentials and optical excitation energies would exhibit the following trend: **Br-AABBBA'-CN** < **Br-BABABA'-CN** < **Br-BBAAAB'-CN**.

As discussed above, to facilitate synthesis and for future incorporation into polymers, we used Br- and -CN end groups. One might suppose, that given the subtle difference in electronic structure between **A** and **B** monomers, the variation in optoelectronic properties is due *solely* to end group effects (e.g., the electron-withdrawing ability of CN on **A'** and **B'**) and not to sequence effects. Instead, sequence generally dominated over end group effects except with the first reduction potential, which was dictated by the terminal cyano group. To further elucidate these effects, calculations were performed on tetramers and hexamers, both with, and without Br- and -CN end groups. While some variations in the exact pattern of sequence effects are found, suggesting both sequence and end groups have influence, the range of computed HOMO energies and gaps was retained (i.e., a span of 0.15 and 0.23 eV for tetramers, with and without end groups, respectively).

Evidence that sequence effects generally dominate over end groups can also be seen through the comparison of the optical spectra of specific compounds. The trimers **Br-ABA'-CN** and **Br-BBA'-CN** have almost identical optical band gaps (2.65 and 2.62 eV, respectively). When these trimers are extended with **B** and **A** monomers to form **Br-ABAB'-CN** and **Br-BBAA'-CN**, however, their band gaps narrow but remain nearly identical despite the addition of different end groups. The tetramers **Br-ABAB'-CN** and **Br-AABB'-CN** have similar spectra (band gaps of 2.58 and 2.55 eV, respectively) while **Br-BAAB'-CN** shows a much higher optical band gap (2.72 eV) despite the fact that all three tetramers have the same **B'-CN** end group. In another example, the pentamers **Br-AABBB'-CN** and **Br-BABAB'-CN** have the same **B'-CN** end group and exhibit an optical gap difference of 0.09 eV. When these pentamers are extended to hexamers by adding an additional **A'-CN** unit to give **Br-AABBBA'-CN** and **Br-BABABA'-CN** the optical gap difference almost *doubles* to 0.17 eV, a clear indication that retaining identical end groups is not sufficient to determine gaps.

The primary trend observed across all properties and the computational results, is that the alternating sequences e.g., **ABABAB** or **BABABA**, are generally neither the highest nor lowest in any category. A secondary widespread trend is that the oligomers that bear **A** monomers in both the first and last positions tend to exhibit smaller HOMO–LUMO gaps, more positive first oxidation potentials, and higher melting points. We also find that among absorption intensities (ϵ), sequences that bear **B** monomers in both the first and last positions (e.g., **Br-BAAB'-CN** or **Br-BABAB'-CN**) exhibit larger extinction coefficients than their counterparts. Although we find these trends, it is important to acknowledge that the use of complex sequences can lead to synergistic effects, and thus unique “outliers”. The use of accurate, reliable computational screening methods makes the identification of these unique sequences practical.

This initial study is particularly promising despite the highly similar electronic characteristics of the two monomers.

Although the differences in the monomers were modest, relative to true donor–acceptor pairs, we find a measurable difference in the sequenced oligomers across a wide range of characteristics. We predict that much stronger sequence effects will be found in systems with greater variation between donor and acceptor monomers, e.g. thiophenes, pyrroles, etc., and are presently pursuing this direction.

Control of sequence provides an entirely new dimension for optimization of conjugated materials. In parallel with the extremely productive strategy of creating novel monomers, sequence engineering offers a pathway to tailor targeted properties using existing, synthetically accessible monomers. Finally, the future correlation of sequence with other properties of interest, e.g., hole mobility, film morphology, and interfacial organization, should allow for the rational design of materials from known monomers that can satisfy the multiplicity of criteria that are necessary for the performance of these materials in real-world photovoltaic applications.

METHODS

Materials. Unless otherwise noted all compounds were purchased from Aldrich. Anhydrous DMF, ⁿBuLi (1.6 M in hexanes), and DIBAL-H (1.0 M in hexanes) were dispensed using air-sensitive techniques. NBS was purchased from Alfa Aesar. Benzoyl peroxide and NBS were stored at –20 °C. KO^tBu was stored in a desiccator over anhydrous CaSO₄. LiCl was purchased from Fisher Scientific and dried at 120 °C for at least 24 h. Anhydrous diethyl ether for lithiation reactions was opened immediately prior to use. Reagent grade THF was used for most reactions; notably the HWE reactions used reagent grade THF. DCM for reactions was purified by distillation from CaH₂ or by passing through a column of alumina. All other reagents and solvents were used as received. Column chromatography was carried out on standard grade silica gel (60 Å pore size, 40–63 μm particle size), which was purchased and used as received. Hexanes, dichloromethane, and ethyl acetate used for column chromatography were purchased and used as received. Melting points for all compounds were determined by DSC and are found in the main text in Table 4, listed as T_{iso} .

Synthesis. General HWE Procedure. Aldehyde (**Br-A-CHO**, **Br-B-CHO**, or **OPV-CHO**) (1 equiv), 4-cyanobenzylphosphonate (**P-A-CN** or **P-B-CN**) (1.5 equiv), and LiCl (2.3 equiv) were dissolved in THF (12 mL per mmol aldehyde) and cooled to 0 °C under N₂. KO^tBu (2.3 equiv) was added portion-wise over 5 min, and the reactions were allowed to come to room temperature overnight with stirring. The reaction mixtures were poured into saturated aqueous NH₄Cl (2.5 mL per mL of THF). The aqueous layers were extracted thrice with EtOAc or CH₂Cl₂ (equal volume). The combined organic layers were dried over MgSO₄, and the solvent was removed *in vacuo*. The residues were purified by column chromatography. Yields and spectroscopic data for specific oligomers can be found in the Supporting Information.

General DIBAL-H Reduction Procedure. OPV nitriles (1 equiv) were dissolved in dry dichloromethane (5 mL per mmol nitrile) and cooled to 0 °C. DIBAL-H (1.0 M in hexanes, 1.1 equiv) was added dropwise. The reaction mixtures were stirred at 0 °C for 1 h. Wet silica (0.4 mL of H₂O and 1.3 g of SiO₂ per mmol of nitrile) was added and the mixture was stirred at 0 °C for 1 h. Then, K₂CO₃ (0.5 g per mmol of nitrile) and MgSO₄ (0.5 g per mmol of nitrile) were added. The mixtures were filtered and the solids washed with dichloromethane. The combined filtrate and washes were reduced in volume *in vacuo*, and the residues were purified by column chromatography, except as noted. Yields and spectroscopic data for specific oligomers can be found in the Supporting Information.

Spectroscopy. NMR Spectroscopy. ¹H (300 and 400 MHz) and ¹³C (75, 100, and 150 MHz) NMR spectra were recorded on Bruker spectrometers. Chemical shifts were referenced to residual ¹H or ¹³C

signals in deuterated solvents (7.27 and 77.0 ppm, respectively, for CHCl_3 and 5.32 and 54.0 ppm, respectively, for CH_2Cl_2).

Mass Spectrometry. HRMS were recorded on EI-quadrupole or ESI-TOF instruments in the Mass Spectrometry Facility of the University of Pittsburgh.

Optical Spectroscopy. UV/vis absorption spectra were recorded in CHCl_3 on a Perkin-Elmer Lambda 9 UV/vis/NIR spectrometer. Solution (CHCl_3) and film emission spectra were recorded on a Varian Cary Eclipse fluorimeter. Films were drop cast on quartz slides from CHCl_3 .

Thermal Analysis. DSC was performed on a Perkin-Elmer Pyris 6 with a heating and cooling rate of $10\text{ }^\circ\text{C}/\text{min}$.

Electrochemistry. Cyclic voltammetry (CV) and differential pulse voltammetry (DPV) were recorded on a CHI Electrochemical Workstation Model 430a (Austin, TX). Data were collected using a three electrode system consisting of a glassy carbon disk (3 mm dia.) as working electrode, a nonaqueous Ag/Ag^+ reference electrode (1 mM AgNO_3 in acetonitrile), and a Pt-wire as auxiliary electrode in 0.1 M Bu_4NPF_6 in THF freshly distilled from sodium. CV were recorded at 100 mV/s. DPV parameters were as follows: scan rate of 25 mV/s, pulse amplitude 0.05 V and pulse period 0.16 s.

Computational Methods. For each oligomer, an initial 3D structure was generated using Open Babel 2.3.0⁶⁷ (accessed through Pybel), followed by a molecular mechanics minimization and stochastic Monte Carlo conformer search using the MMFF94 force field^{68,69} to find a low energy minima conformation. Final geometries were optimized using Gaussian 09⁷⁰ with density functional theory (DFT) B3LYP/6-31G(d)^{71,72} and checked for consistency using Avogadro 1.0.3.⁷³ To match electrochemical experiments, redox potentials were determined using a combination of orbital energies (i.e., vertical ionization potential and electron affinity) and the ΔSCF procedure, taking the adiabatic energy difference between the optimized geometries of neutral and charged species using the conductor polarizable continuum model (C-PCM) model for acetonitrile.⁷⁴ To compare with optical absorptions, excitation energies and oscillator strengths were computed using ZINDO⁷⁵ and TDDFT using the optimized solution geometry of the neutral species using the C-PCM solvation model⁷⁶ for CHCl_3 . Images of molecules and orbitals in the Supporting Information were prepared using Avogadro.

■ ASSOCIATED CONTENT

● Supporting Information

Synthesis of and characterization data for all oligomers; selected ^1H NMR, selected ^{13}C NMR, DPV, CV, DSC, UV-vis spectra, and fluorescence spectra (further NMR spectra available upon request), raw computed DFT orbital eigenvalues; ZINDO and TDDFT optical excitations and oscillator strengths; results of multivariate regressions between computed and experimental properties; and pictures of HOMO and LUMO orbital shapes. This material is available free of charge via the Internet at <http://pubs.acs.org>.

■ AUTHOR INFORMATION

Corresponding Author

*E-mail: (G.R.H.) geoffh@pitt.edu; (T.Y.M.) tmeyer@pitt.edu.

Author Contributions

B.N.N. and S.Z. were coequal in their contributions and should both be considered first authors. B.N.N., T.Y.M., and G.R.H. proposed the project and designed the experiments. B.N.N., S.Z., J.T.A., and P.C.M. performed the synthesis and characterization. C.M.C. and G.R.H. carried out the calculations. B.N.N., S.Z., T.Y.M., and G.R.H. assembled the data and wrote the manuscript.

Notes

The authors declare no competing financial interest.

■ ACKNOWLEDGMENTS

Funding from the NSF (CHE-0809289) and the University of Pittsburgh is acknowledged.

■ REFERENCES

- (1) Blankenship, R. E.; Tiede, D. M.; Barber, J.; Brudvig, G. W.; Fleming, G.; Ghirardi, M.; Gunner, M. R.; Junge, W.; Kramer, D. M.; Melis, A.; Moore, T. A.; Moser, C. C.; Nocera, D. G.; Nozik, A. J.; Ort, D. R.; Parson, W. W.; Prince, R. C.; Sayre, R. T. *Science* **2011**, *332*, 805.
- (2) Facchetti, A. *Chem. Mater.* **2011**, *23*, 733.
- (3) Szarko, J. M.; Guo, J.; Rolczynski, B. S.; Chen, L. X. *J. Mater. Chem.* **2011**, *21*, 7849–7857.
- (4) Zhao, X.; Zhan, X. *Chem. Soc. Rev.* **2011**, *40*, 3728.
- (5) Heeger, A. J. *Chem. Soc. Rev.* **2010**, *39*, 2354.
- (6) Kroon, R.; Lenes, M.; Hummelen, J. C.; Blom, P. W. M.; de Boer, B. *Polym. Rev.* **2008**, *48*, 531.
- (7) Rasmussen, S. C.; Pomerantz, M. In *Handbook of Conducting Polymers*, 3rd ed.; Skotheim, T. A., Reynolds, J. R., Eds.; CRC Press: Boca Raton, FL, 2007; Vol. 1, p 12/1.
- (8) Roncali, J. *Chem. Rev.* **1997**, *97*, 173.
- (9) Grimdale, A. C.; Chan, K. L.; Martin, R. E.; Jokisz, P. G.; Holmes, A. B. *Chem. Rev.* **2009**, *109*, 897.
- (10) Guo, X. G.; Ortiz, R. P.; Zheng, Y.; Hu, Y.; Noh, Y. Y.; Baeg, K. J.; Facchetti, A.; Marks, T. J. *J. Am. Chem. Soc.* **2011**, *133*, 1405.
- (11) Izuhara, D.; Swager, T. M. *J. Mater. Chem.* **2011**, *21*, 3579.
- (12) Choi, S. H.; Frisbie, C. D. *J. Am. Chem. Soc.* **2010**, *132*, 16191.
- (13) Kim, D. H.; Lee, B. L.; Moon, H.; Kang, H. M.; Jeong, E. J.; Park, J. I.; Han, K. M.; Lee, S.; Yoo, B. W.; Koo, B. W.; Kim, J. Y.; Lee, W. H.; Cho, K.; Becerril, H. A.; Bao, Z. *J. Am. Chem. Soc.* **2009**, *131*, 6124.
- (14) Chen, A. C. A.; Culligan, S. W.; Geng, Y.; Chen, S. H.; Klubek, K. P.; Vaeth, K. M.; Tang, C. W. *Adv. Mater.* **2004**, *16*, 783.
- (15) Ellinger, S.; Graham, K. R.; Shi, P.; Farley, R. T.; Steckler, T. T.; Brookins, R. N.; Taranekekar, P.; Mei, J.; Padilha, L. A.; Ensley, T. R.; Hu, H.; Webster, S.; Hagan, D. J.; Van, S. E. W.; Schanze, K. S.; Reynolds, J. R. *Chem. Mater.* **2011**, *23*, 3805.
- (16) Geng, Y.; Chen, A. C. A.; Ou, J. J.; Chen, S. H.; Klubek, K.; Vaeth, K. M.; Tang, C. W. *Chem. Mater.* **2003**, *15*, 4352.
- (17) Henson, Z. B.; Welch, G. C.; van der Poll, T.; Bazan, G. C. *J. Am. Chem. Soc.* **2012**, *134*, 3766.
- (18) Mallet, C.; Savitha, G.; Allain, M.; Kozmik, V.; Svoboda, J.; Frere, P.; Roncali, J. *J. Org. Chem.* **2012**, *77*, 2041.
- (19) Poander, L. E.; Pandey, L.; Barlow, S.; Tiwari, P.; Risko, C.; Kippelen, B.; Bredas, J. L.; Marder, S. R. *J. Phys. Chem. C* **2011**, *115*, 23149.
- (20) Beaujuge, P. M.; Amb, C. M.; Reynolds, J. R. *Acc. Chem. Res.* **2010**, *43*, 1396.
- (21) Jorgensen, M.; Krebs, F. C. *J. Org. Chem.* **2005**, *70*, 6004.
- (22) Horhold, H. H.; Tillmann, H.; Bader, C.; Stockmann, R.; Nowotny, J.; Klemm, E.; Holzer, W.; Penzkofer, A. *Synth. Met.* **2001**, *119*, 199.
- (23) Jian, H. H.; Tour, J. M. *J. Org. Chem.* **2005**, *70*, 3396.
- (24) O'Boyle, N. M.; Campbell, C. M.; Hutchison, G. R. *J. Phys. Chem. C* **2011**, *115*, 16200.
- (25) Badi, N.; Lutz, J.-F. *Chem. Soc. Rev.* **2009**, *38*, 3383.
- (26) Jones, R. *Nat. Nanotechnol.* **2008**, *3*, 699.
- (27) Lutz, J.-F. *Polym. Chem.* **2010**, *1*, 55.
- (28) Copenhafer, J. E.; Walters, R. W.; Meyer, T. Y. *Macromolecules* **2008**, *41*, 31.
- (29) Li, J.; Stayshich, R. M.; Meyer, T. Y. *J. Am. Chem. Soc.* **2011**, *133*, 6910.
- (30) Stayshich, R. M.; Meyer, T. Y. *J. Polym. Sci., Part A: Polym. Chem.* **2008**, *46*, 4704.
- (31) Stayshich, R. M.; Meyer, T. Y. *J. Am. Chem. Soc.* **2010**, *132*, 10920.
- (32) Stayshich, R. M.; Weiss, R. M.; Li, J.; Meyer, T. Y. *Macromol. Rapid Commun.* **2011**, *32*, 220.

- (33) Weiss, R. M.; Jones, E. M.; Shafer, D. E.; Stayshich, R. M.; Meyer, T. Y. *J. Polym. Sci., Part A: Polym. Chem.* **2011**, *49*, 1847.
- (34) Coates, G. W. *Chem. Rev.* **2000**, *100*, 1223.
- (35) Kramer, J. W.; Treitler, D. S.; Dunn, E. W.; Castro, P. M.; Roisnel, T.; Thomas, C. M.; Coates, G. W. *J. Am. Chem. Soc.* **2009**, *131*, 16042.
- (36) Binauld, S.; Damiron, D.; Connal, L. A.; Hawker, C. J.; Drockenmuller, E. *Macromol. Rapid Commun.* **2011**, *32*, 147.
- (37) Ueda, M. *Prog. Polym. Sci.* **1999**, *24*, 699.
- (38) Oppen, K. L.; Wagener, K. B. *J. Polym. Sci., Part A: Polym. Chem.* **2011**, *49*, 821.
- (39) Pfeifer, S.; Lutz, J.-F. *J. Am. Chem. Soc.* **2007**, *129*, 9542.
- (40) Satoh, K.; Matsuda, M.; Nagai, K.; Kamigaito, M. *J. Am. Chem. Soc.* **2010**, *132*, 10003.
- (41) Soeriyadi, A. H.; Boyer, C.; Nystrom, F.; Zetterlund, P. B.; Whittaker, M. R. *J. Am. Chem. Soc.* **2011**, *133*, 11128.
- (42) Tong, X.; Guo, B.-h.; Huang, Y. *Chem. Commun.* **2011**, *47*, 1455.
- (43) Ida, S.; Ouchi, M.; Sawamoto, M. *J. Am. Chem. Soc.* **2010**, *132*, 14748.
- (44) Maddux, T.; Li, W. J.; Yu, L. P. *J. Am. Chem. Soc.* **1997**, *119*, 844.
- (45) Iwadate, N.; Sugimoto, M. *Org. Lett.* **2009**, *11*, 1899.
- (46) Norris, B. N.; Pan, T.; Meyer, T. Y. *Org. Lett.* **2010**, *12*, 5514.
- (47) Krebs, F. C.; Nyberg, R. B.; Jorgensen, M. *Chem. Mater.* **2004**, *16*, 1313.
- (48) Brandt, P.; Norrby, P.-O.; Martin, I.; Rein, T. *J. Org. Chem.* **1998**, *63*, 1280.
- (49) Markiewicz, J. T.; Schauer, D. J.; Lofstedt, J.; Corden, S. J.; Wiest, O.; Helquist, P. *J. Org. Chem.* **2010**, *75*, 2061.
- (50) Hutchison, G. R. *J. Phys. Chem. A* **2002**, *106*, 10596.
- (51) Hutchison, G. R.; Zhao, Y.; Delley, B.; Freeman, A.; Ratner, M.; Marks, T. *Phys. Rev. B* **2003**, *68*, 035204.
- (52) Patra, A.; Wijsboom, Y. H.; Leitus, G.; Bendikov, M. *Chem. Mater.* **2011**, *23*, 896.
- (53) Bredas, J.-L.; Norton, J. E.; Cornil, J.; Coropceanu, V. *Acc. Chem. Res.* **2009**, *42*, 1691.
- (54) Mondal, R.; Ko, S.; Norton, J. E.; Miyaki, N.; Becerril, H. A.; Verploegen, E.; Toney, M. F.; Bredas, J.-L.; McGehee, M. D.; Bao, Z. *J. Mater. Chem.* **2009**, *19*, 7195.
- (55) Hachmann, J.; Olivares-Amaya, R.; Atahan-Evrenk, S.; Amador-Bedolla, C.; Sanchez-Carrera, R. S.; Gold-Parker, A.; Vogt, L.; Brockway, A. M.; Aspuru-Guzik, A. *J. Phys. Chem. Lett.* **2011**, *2*, 2241.
- (56) Perdew, J.; Levy, M. *Phys. Rev. B* **1997**, *56*, 16021.
- (57) Levy, M. *Phys. Rev. A* **1995**, *52*, R4313.
- (58) Zhan, C.; Nichols, J.; Dixon, D. *J. Phys. Chem. A* **2003**, *107*, 4184.
- (59) Rienstra-Kiracofe, J.; Tschumper, G.; Schaefer, H.; Nandi, S.; Ellison, G. *Chem. Rev.* **2002**, *102*, 231.
- (60) Winget, P.; Weber, E.; Cramer, C.; Truhlar, D. G. *Phys. Chem. Chem. Phys.* **2000**, *2*, 1231.
- (61) Jaque, P.; Marenich, A. V.; Cramer, C. J.; Truhlar, D. G. *J. Phys. Chem. C* **2007**, *111*, 5783.
- (62) Kamlet, M.; Abboud, J.; Abraham, M.; Taft, R. *J. Org. Chem.* **1983**, *48*, 2877.
- (63) Sherwood, G. A.; Cheng, R.; Smith, T. M.; Werner, J. H.; Shreve, A. P.; Peteanu, L. A.; Wildeman, J. *J. Phys. Chem. C* **2009**, *113*, 18851.
- (64) So, W. Y.; Hong, J.; Kim, J. J.; Sherwood, G. A.; Chacon-Madrid, K.; Werner, J. H.; Shreve, A. P.; Peteanu, L. A.; Wildeman, J. *J. Phys. Chem. B* **2012**, *116*, 10504.
- (65) Thulstrup, P. W.; Hoffmann, S. V.; Hansen, B. K. V.; Spanget-Larsen, J. *Phys. Chem. Chem. Phys.* **2011**, *13*, 16168.
- (66) Tilley, A. J.; Danczak, S. M.; Browne, C.; Young, T.; Tan, T.; Ghiggino, K. P.; Smith, T. A.; White, J. *J. Org. Chem.* **2011**, *76*, 3372.
- (67) O'Boyle, N. M.; Banck, M.; James, C. A.; Morley, C.; Vandermeersch, T.; Hutchison, G. R. *J. Cheminformatics* **2011**, *3*, 33.
- (68) Halgren, T. *J. Comput. Chem.* **1996**, *17*, 553.
- (69) Halgren, T.; Nachbar, R. *J. Comput. Chem.* **1996**, *17*, 587.
- (70) Gaussian 09, Revision A.2, Frisch, M. J.; Trucks, G. W.; Schlegel, H. B.; Scuseria, G. E.; Robb, M. A.; Cheeseman, J. R.; Scalmani, G.; Barone, V.; Mennucci, B.; Petersson, G. A.; et al. Gaussian, Inc.: Wallingford CT, 2009.
- (71) Becke, A. *J. Chem. Phys.* **1993**, *98*, 5648.
- (72) Lee, C.; Yang, W.; Parr, R. *Phys. Rev. B* **1988**, *37*, 785.
- (73) Hanwell, M. D.; Curtis, D. E.; Lonie, D. C.; Vandermeersch, T.; Zurek, E.; Hutchison, G. R. *J. Cheminf.* **2012**, *4*, 17.
- (74) Tomasi, J.; Mennucci, B.; Cammi, R. *Chem. Rev.* **2005**, *105*, 2999–3093.
- (75) Ridley, J.; Zerner, M. *Theor. Chim. Acta* **1973**, *32*, 111.
- (76) Cossi, M.; Barone, V. *J. Chem. Phys.* **2001**, *115*, 4708.